Physical Chemistry Chemical Physics c1cp20631a

Q1 **Boron and nitrogen-rich carbons from ionic liquid precursors with tailorable surface properties**

Pasquale F. Fulvio, Je Seung Lee,* Richard T. Mayes, Xiqing Wang, Shannon M. Mahurin and Sheng Dai*

Q2

Please check this proof carefully. **Our staff will not read it in detail after you have returned it.** Translation errors between word-processor files and typesetting systems can occur so the whole proof needs to be read. Please pay particular attention to: tabulated material; equations; numerical data; figures and graphics; and references. If you have not already indicated the corresponding author(s) please mark their name(s) with an asterisk. Please e-mail a list of corrections or the PDF with electronic notes attached -- do not change the text within the PDF file or send a revised manuscript.

**Please bear in mind that minor layout improvements, e.g. in line breaking, table widths and graphic placement, are routinely applied to the final version.**

Please note that, in the typefaces we use, an italic vee looks like this: $\nu$, and a Greek nu looks like this: $\nu$.

We will publish articles on the web as soon as possible after receiving your corrections; **no late corrections will be made.**

Please return your **final** corrections, where possible within **48 hours** of receipt, by e-mail to: pccp@rsc.org.

Reprints—Electronic (PDF) reprints will be provided free of charge to the corresponding author. Enquiries about purchasing paper reprints should be addressed via: http://www.rsc.org/publishing/journals/guidelines/paperreprints/. Costs for reprints are below:

| Reprint costs | | |
|---|---|---|
| No of pages | Cost (per 50 copies) | |
| | First | Each additional |
| 2-4 | £225 | £125 |
| 5-8 | £350 | £240 |
| 9-20 | £675 | £550 |
| 21-40 | £1250 | £975 |
| >40 | £1850 | £1550 |
| *Cost for including cover of journal issue:* £55 per 50 copies | | |

Queries are marked on your proof like this Q1, Q2, etc. and for your convenience line numbers are indicated like this 5, 10, 15, ...

| Query reference | Query | Remarks |
|---|---|---|
| Q1 | For your information: You can cite this article before you receive notification of the page numbers by using the following format: (authors), Phys. Chem. Chem. Phys., (year), DOI: 10.1039/c1cp20631a. | |
| Q2 | Please provide a graphical abstract and some text for the contents page. The image can be in colour, at most 8 cm wide by 4 cm high (a CMYK, 600 dpi TIF file, preferably). The descriptive text should be no longer than 30 words. Please ensure that the text fits within the allocated space indicated on the front page of the proof. | |
| Q3 | In the sentence beginning 'External surface...' should 'non-graphitized Cabot BP 280 non-graphitized carbon black as reference' be changed to 'non-graphitized Cabot BP 280, a non-graphitized carbon black, as a reference'? | |
| Q4 | Ref. 26 and 38: Please provide details of the last page number for these articles. | |
| Q5 | Ref. 39: Can this reference be updated yet? | |

PCCP

Dynamic Article Links

Cite this: DOI: 10.1039/c1cp20631a

www.rsc.org/pccp

PAPER

# Boron and nitrogen-rich carbons from ionic liquid precursors with tailorable surface properties†

Pasquale F. Fulvio,[a] Je Seung Lee,*[ab] Richard T. Mayes,[a] Xiqing Wang,‡[a] Shannon M. Mahurin[a] and Sheng Dai*[a]

*Received 5th March 2011, Accepted 12th April 2011*
**DOI: 10.1039/c1cp20631a**

A novel strategy for tailoring the adsorption and structural properties of ionic liquid derived carbons has been developed. By changing the carbonization temperature and ratios of ionic liquids (ILs) containing a cross-linkable anion, such as 1-butyl-3-methylimidazolium tricyanomethanide [BMIm][C(CN)$_3$] and 1-ethyl-3-methylimidazolium tetracyanoborate [EMIm][B(CN)$_4$], boron and nitrogen-rich carbons with slit-like pores and specific surface areas exceeding 500 m$^2$ g$^{-1}$ have been prepared. Furthermore, the nitrogen-rich carbons exhibit high adsorption capacity for $CO_2$ adsorption and selectivity for $CO_2/N_2$ separation.

## Introduction

Porous carbon materials have been used as catalyst supports, gas sorbents and as electrodes for their typically large surface areas, good chemical and thermal stabilities, and high electronic conductivity.[1–7] In addition, carbons doped with heteroatoms such as nitrogen have been largely investigated for the oxygen reduction reaction in fuel cells, as supercapacitors, and as highly selective gas separation membranes.[8–10] To date, several types of carbons have been prepared from carbonization and activation of biomass sources such as coconut[11] and most recently prawn shells.[12] The latter, however, limited these materials for most applications due to difficulties found in controlling the final porosity, doping, the presence of undesirable impurities and in graphitizing most natural carbon sources.

In order to overcome these problems, carbon materials with well-defined micro, meso and macropores have been prepared by hard[13–15] and soft-templating techniques.[7,16–20] In the hard templating method, the surfaces and pores of materials such as silica colloidal spheres,[2] silica colloidal crystals[21] and ordered mesoporous silicas[13–15] are filled with a carbon precursor. After carbonization, the template is removed and pores are obtained as inverse replicas of the template structure. This method not only allows for the control over the size and geometry of mesopores, but also on the presence of heteroatoms, *i.e.* boron,[22,23] nitrogen[24–27] and sulfur,[28] by selecting the proper carbon precursors. Nevertheless, this method requires the preparation of templates, adding time and increased costs to the preparation of the final carbon materials, while also requiring the use of sodium hydroxide or toxic hydrofluoric acid to remove the templates. Complementary to the hard-templating method, the soft-templating synthesis of mesoporous carbons offers several advantanges in terms of cost and synthesis time. By the organic–organic self-assembly of triblock-copolymers and phenolic resins, followed by carbonization, mesoporous carbons are obtained.[7,16–20] During the thermal treatments, the phenolic resins are converted into carbons, whereas the triblock copolymers are thermally unstable and decompose, generating the mesopores in these carbon materials. As in the hard-templated carbons, heteroatom-doped carbons could be obtained by using organic precursors with functional groups containing nitrogen[29–31] and even boron and phosphorus by adding mixtures of boric and phosphoric acids to the syntheses gels.[32] For both methods however, the large extent of the thermal decomposition of the organic functional groups during thermal treatments above 400 °C resulted in carbons with low heteroatom yields. For most applications, such as catalysis and separations, higher amounts of accessible heteroatoms are desired. In order to increase the number of active sites on these carbons, activation with ammonia and acetonitrile vapors has been proposed,[9,10] but this procedure requires the use of both toxic substances while nitrogen levels were still below 10 wt%.

In an attempt to increase the nitrogen contents, carbon materials with surface areas, up to 3300 m$^2$ g$^{-1}$, dynamic polymerization of organic nitriles were performed with zinc(II)

[a] *Chemical Sciences Division, Oak Ridge National Laboratory, 1 Bethel Valley Road, Oak Ridge, TN 37831, USA. E-mail: dais@ornl.gov; Fax: +1 865 576 5235; Tel: +1 865 576 7307*
[b] *Department of Chemistry, Kyung Hee University, 1 Hoegi-dong, Dongdaemoon-gu, Seoul 130-701, Korea. E-mail: leejs70@khu.ac.kr; Fax: +82 2 966 3701; Tel: +82 2 961 0458*

† Electronic supplementary information (ESI) available: Tables S1 and S2 containing adsorption/physical properties and EDX elemental analysis results for carbons, respectively, and Fig. S1 with nitrogen adsorption isotherms at −196 °C for carbonaceous materials prepared at various temperatures and different mixtures of TSILs. See DOI: 10.1039/c1cp20631a

‡ Nanotek Instruments, Inc., Dayton, OH 45404, USA.

chloride ($ZnCl_2$) as the catalyst at 400 °C.[33] Final materials exhibited C/N molar ratios of up to 4 at 400 °C. However, the latter values dramatically increased up to 17 after carbonizations at 700 °C as a result of the decomposition of nitrile groups. And even though this method did not require the use of templates, pressurized chemical reactors were necessary to prevent the loss of the monomer gas. Also, treatments with inorganic acids were required to remove the $ZnCl_2$ used from the polymeric materials. Graphitic carbon nitride ($g$-$C_3N_4$) structures have also been reported according to this method. The actual C/N molar ratios were approximately 5, indicating the loss of large quantities of nitrogen during pyrolysis at high temperature and final surface areas were in the range of 86 to 439 $m^2\ g^{-1}$ when using silica templates.[34]

Recently, our group[35–37] and others[38,39] have successfully demonstrated the facile preparation of nitrogen-rich micro and mesoporous carbons *via* an ionothermal synthesis involving task specific ionic liquids (TSILs).

In the latter, ILs with cross-linkable cations, or anions (TSILs) were shown to form nitrogen-rich nanoporous carbons, with the size of pores dictated by the size of the cation, or anion that does not cross-link, but is thermally decomposed instead. This self-templated process did not require extreme hydrothermal conditions, since most ionic liquids (ILs) and TSILs have negligible vapor pressures, wide liquid temperature ranges and high chemical and thermal stabilities. In previous studies, we demonstrated that TSILs with either anions or cations having nitrile functional groups were cross-linked and carbonized during thermal treatments at 800 °C in ambient pressure. In case of TSILs containing cross-linkable cations, the nitrogen contents were 2–3 wt% and with surface areas up to 781 $m^2\ g^{-1}$, and the porosity was easily controlled by the size of the anion of TSIL. Whereas products from TSILs containing cross-linkable anions also showed good correlation between the porosity and cation size, but surface areas were still below 90 $m^2\ g^{-1}$. The C/N molar ratios were as low as 2.8, indicating that anions with different cross-linkable functional groups may lead to nitrogen-rich carbonaceous materials,[35,36] making these systems interesting for further investigation to improve their final surface properties.

In the present work, we report the use of mixtures of two TSILs containing different anions bearing multiple cross-linkable components, as shown in Fig. 1, TSILs with 3 nitrile groups in $[C(CN)_3]^-$ and four nitrile groups in $[B(CN)_4]^-$. The latter TSILs are expected to allow the formation of 3-dimensional connected intermediate carbonaceous frameworks, as illustrated in Fig. 2,

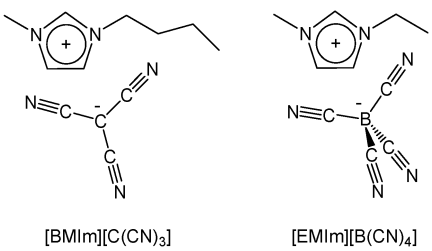


**Fig. 1** Two dialkylimidazolium TSILs bearing nitrile-functionalized group.

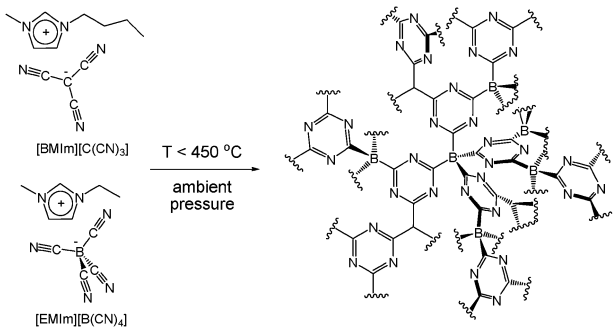


**Fig. 2** Proposed reaction scheme of the trimerization of a nitrile-containing anion, leading to the formation of a 3-dimensional extended framework.

thus favoring the formation of boron and nitrogen-rich carbons with larger specific surface areas than previously reported. By changing the ratios of the two TSILs, non-porous samples, and carbons with some accessible micropores and broad distributions of slit-like mesopores were obtained with surface areas exceeding 500 $m^2\ g^{-1}$. Large B and N contents were found for these materials even after carbonizations at 800 °C. Furthermore, the final carbon materials exhibited reversible high adsorption capacities for the room temperature, high pressure adsorption of carbon dioxide ($CO_2$) compared to nitrogen ($N_2$). The latter results represent a major advance for the future ionothermal synthesis of nanoporous carbons with surface functional groups for gas storage and selective membranes for gas separations.

## Experimental

### Materials

1-Butyl-3-methylimidazolium tricyanomethanide ([BMIm]-[$C(CN)_3$]) and 1-ethyl-3-methylimidazolium tetracyanoborate ([EMIm][$B(CN)_4$]) were purchased from Merck Chemicals and used without further purification. Fig. 1 shows the chemical structures of [BMIm][$C(CN)_3$] and [EMIm][$B(CN)_4$]. Nitrogen and carbon dioxide gas cylinders (99.99% purity) were obtained from Air Liquide.

### Carbonization of liquid precursors

Carbonization of TSILs was carried out by introducing 0.5 g of a particular IL or IL mixture with proper ratio into an alumina crucible in a horizontal quartz tube furnace. The pure TSILs and mixtures were then heated at 10 °C per min to the final temperature of 450, 550, 800 or 900 °C for 1 h in flowing nitrogen (100 $cm^3\ min^{-1}$).

### Characterization

Nitrogen adsorption isotherms were recorded on a Micromeritics TriStar analyzer at −196 °C. Prior to measurement, the samples were outgassed in flowing $N_2$ at 150 °C for 3 h. The specific surface areas were calculated using the Brunauer–Emmett–Teller (BET) method from the nitrogen adsorption data in the relative range ($p/p_0$) of 0.06–0.20.[40] External surface areas and micropore contents were calculated Q3


This journal is © the Owner Societies 2011

from $\alpha_S$-plots and using a standard adsorption isotherm for a non-graphitized Cabot BP 280 non-graphitized carbon black as reference.[41]

High-pressure $CO_2$ and $N_2$ adsorption were measured using an Intelligent Gravimetric Analyzer (Hiden Analytical Limited, UK). In a typical experiment, approximately 80 mg of material were loaded into a quartz bucket cell and evacuated to 0.1 atm for 6 h at 150 °C. All measurements were acquired at room temperature. The mass uptake (corrected for buoyancy) was then measured as a function of pressure up to a final pressure of 10 atm to obtain the adsorption isotherm. Desorption isotherms were subsequently acquired by measuring the mass as a function of decreasing pressure to ensure that the adsorption behavior was reversible and to test for hysteresis effects. Energy-dispersive X-ray spectroscopy (EDX) measurements were acquired with a JEOL-6060 scanning electron microscope using the electron energy of 15 kV.

## Results and discussion

### Carbon yields of TSILs

As shown in Table 1 and Table S1 in the ESI†, carbon yields are much lower than the corresponding theoretical values calculated on the basis of overall carbon contents in each IL or IL mixture. However, the carbon yield values agree well with the corresponding theoretical values calculated on the basis of carbon contents of anion(s) in each TSIL or TSIL mixture. As reported previously, the cations without cross-linkable functional groups decompose during thermal treatments,[35,36] and the final carbon yields result from the TSIL anions. Similar to the aromatic nitriles,[33,42] cyanamide,[43] and acetylenes,[44] the polymerization of $[C(CN)_3]^-$ and $[B(CN)_4]^-$ in the temperature range of 300 to 450 °C is expected to proceed by a cyclotrimerization reaction forming condensed carbonaceous materials,[33] as shown in Fig. 2. During the cyclotrimerization reaction, part of the TSIL cations may be confined within the 3-dimensional carbonaceous frameworks, slightly increasing the carbon yields from the theoretical values based exclusively on the anions. For all experimental values, the carbon yields include other elements such as boron, nitrogen and oxygen contents identified by EDX analysis, see Table S2 in ESI.† Thus, these refer to the actual yield of solid matter obtained from the carbonization of TSILs.

### Porosity control of carbonaceous material

The $N_2$ adsorption isotherms for the carbons derived from pure TSILs and mixtures at 800 °C are shown in Fig. 3 and Fig. S1 in ESI.† These are type II with H-3 hysteresis loops, typical of solids with large slit-like mesopores formed by particle aggregates.[40] The specific surface areas of samples from pure ionic liquids were approximately 13 and 68 $m^2\ g^{-1}$ for $[EMIm][B(CN)_4]$ and $[BMIm][C(CN)_3]$, respectively (see Table 1). Such difference may result from the higher degree of cross-linking from the $[B(CN)_4]^-$ anion and consequently forming larger carbon particles and with more dense walls compared to the $[C(CN)_3]^-$ anion. For the $[BMIm][C(CN)_3]/[EMIm][B(CN)_4]$ ratio of 2/1, the surface area increased to approximately 120 $m^2\ g^{-1}$. When the ratio of $[EMIm][B(CN)_4]$ was further increased, the surface area of the resulting carbon was above 180 $m^2\ g^{-1}$ as a result of the better cross-linking induced by the $[B(CN)_4]^-$, possibly limiting the final particle size and also forming some accessible micropores. The latter hypothesis is supported by the small increments in the calculated micropore volumes (see Table 1), which increased from ~0.005 $cm^3\ g^{-1}$ for $[EMIm][B(CN)_4]$ to 0.09 $cm^3\ g^{-1}$ for $[BMIm][C(CN)_3]/[EMIm][B(CN)_4]$ of 1 : 2.

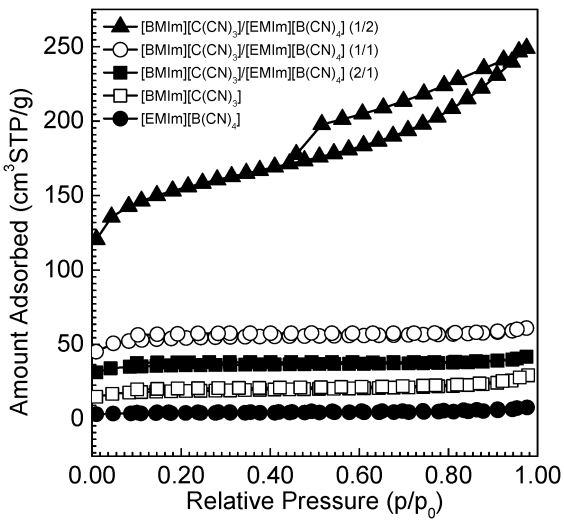


**Fig. 3** Nitrogen sorption isotherms of carbon materials derived from pure $[BMIm][C(CN)_3]$ and $[EMIm][B(CN)_4]$ and from mixtures of both ILs after carbonization at 800 °C for 1 h in a flowing nitrogen atmosphere.

**Table 1** Elemental analysis composition from EDX analysis and specific surface areas of final porous carbons prepared from TSIL mixtures after carbonization at 800 °C in flowing nitrogen

| Sample | | C yield exp. (wt%) | C yield theor. (wt%)[a] | C yield theor. (wt%)[b] | $S_{BET}$/ $m^2\ g^{-1}$ [c] | $V^{\alpha}_{mi}$/ $cm^3\ g^{-1}$ [d] | $S^{\alpha}_{mi}$/ $m^2\ g^{-1}$ [e] | $V_{SP}$/ $cm^3\ g^{-1}$ [f] |
|---|---|---|---|---|---|---|---|---|
| $[BMIm][B(CN)_4]$ | $[EMIm][C(CN)_3]$ | | | | | | | |
| 1 | 0 | 22.5 | 62.9 | 20.1 | 65 | 0.027 | 9.71 | 0.04 |
| 0 | 1 | 37.7 | 53.1 | 21.3 | 14 | 0.005 | 2.66 | 0.01 |
| 1 | 1 | 29.2 | 58.0 | 20.7 | 188 | 0.081 | 7.76 | 0.09 |
| 1 | 2 | 29.6 | 56.4 | 20.9 | 537 | 0.09* | 127* | 0.25 |
| 2 | 1 | 28.9 | 59.6 | 20.5 | 124 | 0.054 | 4.93 | 0.06 |

[a] Theoretical values of C% for each precursor TSIL. [b] Theoretical values of C% for each precursor TSIL based on anion. [c] Specific surface area calculated using the BET equation in the relative pressure range of 0.06–0.20. [d] Micropore volume. [e] Micropore surface area calculated in the $\alpha_S$-plot range of 0.9–1.2 (*0.8–1.0). [f] Single point pore volume from adsorption isotherms at $p/p_0$ ~0.92.

**Table 2** Nitrogen adsorption at −196 °C for the carbons prepared using [BMIm][C(CN)$_3$]/[EMIm][B(CN)$_4$] of 1/2 carbonized at various temperatures

| T/°C[a] | $S_{BET}$/m$^2$ g$^{-1}$ [b] | $V_{SP}$/cm$^3$ g$^{-1}$ [c] | $V_t^{\alpha}$/cm$^3$ g$^{-1}$ [d] | $V_{mi}^{\alpha}$/cm$^3$ g$^{-1}$ [e] | $S_{mi}^{\alpha}$/m$^2$ g$^{-1}$ [f] | $S_{ext}^{\alpha}$/m$^2$ g$^{-1}$ [g] |
|---|---|---|---|---|---|---|
| 450 | 314 | 0.25 | 0.24 | 0.09 | 127 | 14.0 |
| 550 | 381 | 0.30 | 0.28 | 0.11 | 141 | 22.5 |
| 800 | 528 | 0.36 | 0.35 | 0.17 | 154 | 13.0 |
| 900 | 282 | 0.23 | 0.22 | 0.07 | 131 | 10.0 |

[a] Carbonization temperature. [b] Specific surface area calculated using the BET equation in the relative pressure range of 0.06–0.20. [c] Single point pore volume from adsorption isotherms at $p/p_0$ ~0.92. [d] Total pore volume calculated in the $\alpha_S$-plot range of 2.5–4.5. [e] Micropore volume. [f] Micropore surface area calculated in the $\alpha_S$-plot range of 0.8–1.0. [g] External surface area calculated within the $\alpha_S$-plot range of 2.5–4.5.

### Temperature dependence of porosity

For the series of samples with the largest pore volumes, those obtained from a 1/2 ratio mixture of [BMIm][C(CN)$_3$]/[EMIm][B(CN)$_4$], the effect of carbonization temperature was further investigated and the adsorption data results are summarized in Table 2. The specific surface areas of the carbonaceous samples gradually increase after carbonizations at 450 °C to 800 °C, *viz*. from 314 to 528 m$^2$ g$^{-1}$. Also the total and micropore volumes follow the same trend. Once the temperature was raised to 900 °C, those parameters decreased as a result of the further densification of the carbon structure. This densification is accompanied by decrease in the nitrogen contents of these samples carbonized from 450 to 900 °C. For this series, the amounts of nitrogen went from approx. 9.4 wt% for samples carbonized at 450 °C, down to 4.0 wt% after treatments at 900 °C, as shown in Table S2 in ESI.† Also carbon contents were lower after heating at 900 °C, whereas boron contents were over 23 wt% for all carbonizations above 550 °C.

### Carbon dioxide adsorption and selectivity properties

High-pressure $CO_2$ and $N_2$ adsorptions for [BMIm][C(CN)$_3$] and [BMIm][C(CN)$_3$]/[EMIm][B(CN)$_4$] = 1/2 samples carbonized at 800 °C are shown in Fig. 4.

While ionic liquids are actively explored for $CO_2$ sequestration,[45] most well known conventional $CO_2$ absorbents are alkanolamines such as monoethanolamine. However, alkanolamines suffer from several disadvantages including the corrosiveness of alkanolamine/water solutions, the large amount of energy consumed during regeneration, and the loss of alkanolamines during the latter process.[46,47] To overcome these drawbacks, solid adsorbents such as zeolites and activated carbons have been studied.[48–50] Recently, mesoporous silica containing surface amine functional groups that can strongly interact with $CO_2$ have also been investigated.[51] For the latter silica materials, the $CO_2$ uptake capacity was of 1.4 mmol g$^{-1}$, corresponding to 6.2 wt% $CO_2$ at 1 atm. Though this $CO_2$ uptake capacity is still smaller than previous results reported for zeolite 13X and for activated carbons, it provided the first insights for enhancing the $CO_2$ reversible adsorption capacity for a solid by introducing surface functional groups. Similarly, materials significantly lighter than silica, such as carbons, may have their surface properties modified to enhance their affinity and selectivity for gas storage and separations.

For the carbons reported herein, while low $N_2$ adsorption properties are exhibited, the material derived from the IL mixture demonstrates slightly higher $N_2$ adsorption possibly because of its much larger surface area. No hysteresis was observed during $CO_2$ or $N_2$ desorption from these materials. At lower pressures, the carbon from the TSIL mixture adsorbed more $CO_2$ than the carbon from [BMIm][C(CN)$_3$] only, possibly because of its much larger surface area. Interestingly, above 2 atm, the carbon derived from [BMIm][C(CN)$_3$] which has a lower surface area shows higher $CO_2$ adsorption than the carbon derived from [BMIm][C(CN)$_3$]/[EMIm][B(CN)$_4$] of 1/2. The calculated $CO_2$ uptake of carbons derived from [BMIm][C(CN)$_3$]/[EMIm][B(CN)$_4$] of 1/2 at 1 and 10 atm were 1.73 and 3.30 mmol g$^{-1}$, respectively. Whereas for carbons derived from [BMIm][C(CN)$_3$], also at 1 and 10 atm, this was 1.47 and 4.87 mmol g$^{-1}$, respectively. The carbon derived from [BMIm][C(CN)$_3$]/[EMIm][B(CN)$_4$] = 1/2 also shows decreasing $CO_2/N_2$ selectivity from 3.76 at 1 atm to 3.55 at 10 atm. However, the carbon derived from [BMIm][C(CN)$_3$] shows increasing selectivity as the pressure is raised from 1 to 10 atm. At 10 atm, the $CO_2/N_2$ selectivity was 5.87, compared to 3.97 at 1 atm. While [BMIm][C(CN)$_3$]/[EMIm][B(CN)$_4$] = 1/2 carbon material has larger adsorption capacity than [BMIm][C(CN)$_3$] carbon, the latter has approximately 4 times the nitrogen content of the former based on EDX analysis (see Table S2, ESI†). The results for [BMIm][C(CN)$_3$] derived carbons were also superior to those reported for amino-rich glucose derived carbons.[51]

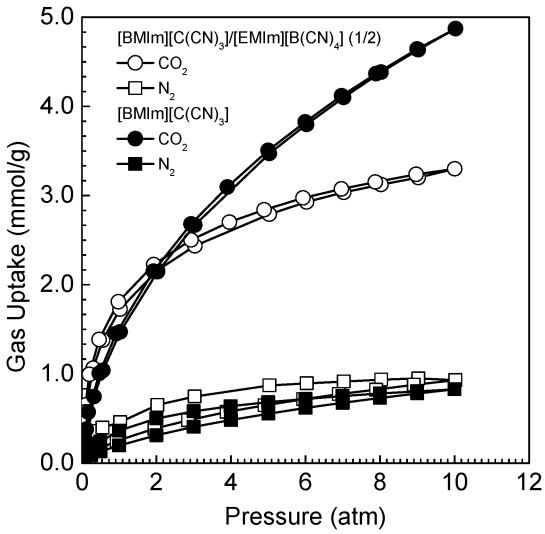


**Fig. 4** $CO_2$ and $N_2$ adsorption-desorption isotherms as a function of pressure for the carbons from [BMIm][C(CN)$_3$] and [BMIm][C(CN)$_3$]/[EMIm][B(CN)$_4$] = 1/2.


This journal is © the Owner Societies 2011

Recently, nitrogen-doped carbon nanotubes (CNTs) have also been investigated for $CO_2$ adsorption.[52] In this work, nitrogen-doped CNTs with large nitrogen contents and low surface areas, exhibit higher $CO_2$ adsorption capacity than other nitrogen-doped carbon nanotubes with larger surface areas and lower nitrogen contents. While the latter results have not been fully understood, nitrogen atoms in carbon frameworks have been known to generate a net positive charge on adjacent carbon atoms due to electronegativity differences between both elements. This positive charge on the carbon may be responsible for the strong interaction with $CO_2$ molecules.[51,52]

Similarly, the presence of relatively high nitrogen contents in our carbons induce the interaction of $CO_2$ molecules, despite of the much lower surface areas than those of activated carbons. However, other than modifying the adsorption properties of the final carbons, the role of boron in the $CO_2$ and $N_2$ uptake at pressures above 2 atm remains unclear and is the focus of future work.

## Conclusions

The synthesis of boron and nitrogen-rich carbons using two TSILs containing cross-linkable anions, namely [BMIm]-[$C(CN)_3$] and [EMIm][$B(CN)_4$], at ambient pressure was reported. The porosity was controlled by varying the ratio of the IL mixture and pyrolysis temperature. The surface areas of carbonaceous materials increased proportionally from the pure [BMIm][$C(CN)_3$] to various added amounts of [EMIm][$B(CN)_4$], with a maximum surface area of 528 $m^2$ $g^{-1}$ found for the [BMIm][$C(CN)_3$]/[EMIm][$B(CN)_4$] of 1/2 carbonized at 800 °C. Furthermore, these newly synthesized carbons are promising for the applications such as $CO_2$ sequestration with high selectivity for $CO_2/N_2$ separation.

## Acknowledgements

J.S.L. was financially supported by a grant from the Fundamental R&D Program for Core Technology of Materials funded by the Ministry of Knowledge Economy, Republic of Korea. X.W. and S.D. were supported by the Division of Chemical Sciences, Geosciences, and Biosciences, Office of Basic Energy Sciences, U. S. Department of Energy, under contract DE-AC05-00OR22725 with Oak Ridge National Laboratory, managed and operated by UT-Battelle, LLC. R. T. M. was supported by the U. S. DOE Office of Energy Efficiency and Renewable Energy (EERE). P.F.F. and S.D. were supported as part of the Fluid Interface Reactions, Structures and Transport (FIRST) Center, an Energy Frontier Research Center funded by the U. S. Department of Energy, Office of Science, Office of Basic Energy Sciences under contract DE-AC05-OR22725 with Oak Ridge National Laboratory, managed and operated by UT-Battelle, LLC.

## Notes and references

1 S. H. Joo, S. J. Choi, I. Oh, J. Kwak, Z. Liu, O. Terasaki and R. Ryoo, *Nature*, 2001, **412**, 169–172.
2 Z. J. Li and M. Jaroniec, *Anal. Chem.*, 2004, **76**, 5479–5485.
3 A. H. Lu, A. Kiefer, W. Schmidt and F. Schuth, *Chem. Mater.*, 2004, **16**, 100–103.
4 W. Yantasee, Y. H. Lin, G. E. Fryxell, K. L. Alford, B. J. Busche and C. D. Johnson, *Ind. Eng. Chem. Res.*, 2004, **43**, 2759–2764.
5 T. W. Kim, P. W. Chung, I. I. Slowing, M. Tsunoda, E. S. Yeung and V. S. Y. Lin, *Nano Lett.*, 2008, **8**, 3724–3727.
6 C. D. Liang, Z. J. Li and S. Dai, *Angew. Chem., Int. Ed.*, 2008, **47**, 3696–3717.
7 Y. Wan, Y. F. Shi and D. Y. Zhao, *Chem. Mater.*, 2008, **20**, 932–945.
8 K. P. Gong, F. Du, Z. H. Xia, M. Durstock and L. M. Dai, *Science*, 2009, **323**, 760–764.
9 X. Q. Wang, J. S. Lee, Q. Zhu, J. Liu, Y. Wang and S. Dai, *Chem. Mater.*, 2010, **22**, 2178–2180.
10 S. M. Mahurin, J. S. Lee, X. Wang and S. Dai, *J. Membr. Sci.*, 2011, **368**, 41–47.
11 A. R. Mohamed, M. Mohammadi and G. N. Darzi, *Renewable Sustainable Energy Rev.*, 2010, **14**, 1591–1599.
12 R. J. White, M. Antonietti and M. M. Titirici, *J. Mater. Chem.*, 2009, **19**, 8645–8650.
13 S. Jun, S. H. Joo, R. Ryoo, M. Kruk, M. Jaroniec, Z. Liu, T. Ohsuna and O. Terasaki, *J. Am. Chem. Soc.*, 2000, **122**, 10712–10713.
14 R. Ryoo, S. H. Joo, M. Kruk and M. Jaroniec, *Adv. Mater.*, 2001, **13**, 677–681.
15 R. Ryoo, S. H. Joo and S. Jun, *J. Phys. Chem. B*, 1999, **103**, 7743–7746.
16 X. Q. Wang, C. D. Liang and S. Dai, *Langmuir*, 2008, **24**, 7500–7505.
17 C. D. Liang and S. Dai, *J. Am. Chem. Soc.*, 2006, **128**, 5316–5317.
18 C. D. Liang, K. L. Hong, G. A. Guiochon, J. W. Mays and S. Dai, *Angew. Chem., Int. Ed.*, 2004, **43**, 5785–5789.
19 Y. Meng, D. Gu, F. Q. Zhang, Y. F. Shi, H. F. Yang, Z. Li, C. Z. Yu, B. Tu and D. Y. Zhao, *Angew. Chem., Int. Ed.*, 2005, **44**, 7053–7059.
20 S. Tanaka, N. Nishiyama, Y. Egashira and K. Ueyama, *Chem. Commun.*, 2005, 2125–2127.
21 K. P. Gierszal and M. Jaroniec, *J. Am. Chem. Soc.*, 2006, **128**, 10026–10027.
22 A. Vinu, T. Mori and K. Ariga, *Sci. Technol. Adv. Mater.*, 2006, **7**, 753–771.
23 A. Vinu, M. Terrones, D. Golberg, S. Hishita, K. Ariga and T. Mori, *Chem. Mater.*, 2005, **17**, 5887–5890.
24 A. Vinu, S. Anandan, C. Anand, P. Srinivasu, K. Ariga and T. Mori, *Microporous Mesoporous Mater.*, 2008, **109**, 398–404.
25 M. Kruk, K. M. Kohlhaas, B. Dufour, E. B. Celer, M. Jaroniec, K. Matyjaszewski, R. S. Ruoff and T. Kowalewski, *Microporous Mesoporous Mater.*, 2007, **102**, 178–187.
26 Y. D. Xia and R. Mokaya, *Adv. Mater*, 2004, **16**, 1553–+. Q4
27 A. B. Fuertes and T. A. Centeno, *J. Mater. Chem.*, 2005, **15**, 1079–1083.
28 Y. S. Shin, G. Fryxell, W. Y. Um, K. Parker, S. V. Mattigod and R. Skaggs, *Adv. Funct. Mater.*, 2007, **17**, 2897–2901.
29 J. P. Yang, Y. P. Zhai, Y. H. Deng, D. Gu, Q. Li, Q. L. Wu, Y. Huang, B. Tu and D. Y. Zhao, *J. Colloid Interface Sci.*, 2010, **342**, 579–585.
30 C. M. Feng, H. X. Li and Y. Wan, *J. Nanosci. Nanotechnol.*, 2009, **9**, 1558–1563.
31 K. Kailasam, Y. S. Jun, P. Katekomol, J. D. Epping, W. H. Hong and A. Thomas, *Chem. Mater.*, 2010, **22**, 428–434.
32 X. C. Zhao, A. Q. Wang, J. W. Yan, G. Q. Sun, L. X. Sun and T. Zhang, *Chem. Mater.*, 2010, **22**, 5463–5473.
33 P. Kuhn, A. Forget, D. S. Su, A. Thomas and M. Antonietti, *J. Am. Chem. Soc.*, 2008, **130**, 13333–13337.
34 A. Thomas, A. Fischer, F. Goettmann, M. Antonietti, J. O. Muller, R. Schlogl and J. M. Carlsson, *J. Mater. Chem.*, 2008, **18**, 4893–4908.
35 J. S. Lee, X. Q. Wang, H. M. Luo, G. A. Baker and S. Dai, *J. Am. Chem. Soc.*, 2009, **131**, 4596–4597.
36 J. S. Lee, X. Q. Wang, H. M. Luo and S. Dai, *Adv. Mater.*, 2010, **22**, 1004–1007.
37 X. Q. Wang and S. Dai, *Angew. Chem., Int. Ed.*, 2010, **49**, 6664–6668.
38 J. P. Paraknowitsch, J. Zhang, D. S. Su, A. Thomas and M. Antonietti, *Adv. Mater.*, 2010, **22**, 87–+.

Q5 39 L. Zhao, Y. S. Hu, H. Li, Z. X. Wang and L. Q. Chen, *Adv. Mater*, 2011, DOI: 10.1002/adma.201003294.
40 M. Kruk and M. Jaroniec, *Chem. Mater.*, 2001, **13**, 3169–3183.
41 M. Kruk, M. Jaroniec and K. P. Gadkaree, *J. Colloid Interface Sci.*, 1997, **192**, 250–256.
42 P. Kuhn, M. Antonietti and A. Thomas, *Angew. Chem., Int. Ed.*, 2008, **47**, 3450–3453.
43 M. J. Bojdys, J. O. Muller, M. Antonietti and A. Thomas, *Chem.–Eur. J.*, 2008, **14**, 8177–8182.
44 Y. Shin, G. E. Fryxell, C. A. Johnson and M. M. Haley, *Chem. Mater.*, 2008, **20**, 981–986.
45 J. F. Brennecke and B. E. Gurkan, *J. Phys. Chem. Lett.*, 2010, **1**, 3459–3464.
46 T. L. Donaldson and Y. N. Nguyen, *Ind. Eng. Chem. Fundam.*, 1980, **19**, 260–266.
47 E. D. Bates, R. D. Mayton, I. Ntai and J. H. Davis, *J. Am. Chem. Soc.*, 2002, **124**, 926–927.
48 R. V. Siriwardane, M.-S. Shen, E. P. Fisher and J. A. Poston, *Energy Fuels*, 2001, **15**, 279–284.
49 P. J. E. Harlick and F. H. Tezel, *Microporous Mesoporous Mater.*, 2004, **76**, 71–79.
50 R. S. Pillai, S. A. Peter and R. V. Jasra, *Microporous Mesoporous Mater.*, 2008, **113**, 268–276.
51 G. Y. Zhao, B. Aziz and N. Hedin, *Appl. Energy*, 2010, **87**, 2907–2913.
52 Y. Shen and J. Bai, *Chem. Commun.*, 2010, **46**, 1308–1310.


This journal is © the Owner Societies 2011